ISSN 1674-1056
http://cpb.iphy.ac.cn
http://iopscience.iop.org/cpb
中国物理 B
Chinese Physics
中国物理 Chinese Physics B

Graphene-like Be_3X_2 (X=C, Si, Ge, Sn): A new family of two-dimensional topological insulators

Lingling Song(宋玲玲), Lizhi Zhang(张礼智), Yurou Guan(官雨柔), Jianchen Lu(卢建臣), Cuixia Yan(闫翠霞), Jinming Cai(蔡金明)

Citation: Chin. Phys. B . 2019, 28(3): 037101. **doi:** 10.1088/1674-1056/28/3/037101
Journal homepage: http://cpb.iphy.ac.cn; http://iopscience.iop.org/cpb

What follows is a list of articles you may be interested in

Exploration of the structural and optical properties of a red-emitting phosphor $K_2TiF_6:Mn^{4+}$

Xi-Long Dou(豆喜龙), Xiao-Yu Kuang(邝小渝), Xin-Xin Xia(夏欣欣), Meng Ju(巨濛)
Chin. Phys. B . 2019, 28(1): 017107. **doi:** 10.1088/1674-1056/28/1/017107

Antiferromagnetic–ferromagnetic transition in zigzag graphene nanoribbons induced by substitutional doping

Shenyuan Yang(杨身园), Jing Li(李静), Shu-Shen Li(李树深)
Chin. Phys. B . 2018, 27(11): 117102. **doi:** 10.1088/1674-1056/27/11/117102

First-principles study on the mechanics, optical, and phonon properties of carbon chains

Jin-Ping Li(李金平), Song-He Meng(孟松鹤), Han-Tao Lu(陆汉涛), Takami Tohyama(遠山貴巳)
Chin. Phys. B . 2018, 27(11): 117101. **doi:** 10.1088/1674-1056/27/11/117101

Effect of Mn doping on mechanical properties and electronic structure of WCoB ternary boride by first-principles calculations

Tong Zhang(张桐), Hai-Qing Yin(尹海清), Cong Zhang(张聪), Xuan-Hui Qu(曲选辉), Qing-Jun Zheng(郑清军)
Chin. Phys. B . 2018, 27(10): 107101. **doi:** 10.1088/1674-1056/27/10/107101

Ferromagnetic-insulators-modulated transport properties on the surface of a topological insulator

Guo Jun-Ji, Liao Wen-Hu
Chin. Phys. B . 2014, 23(6): 067104. **doi:** 10.1088/1674-1056/23/6/067104

Graphene-like Be_3X_2 (X = C, Si, Ge, Sn): A new family of two-dimensional topological insulators*

Lingling Song(宋玲玲)[1], Lizhi Zhang(张礼智)[2], Yurou Guan(官雨柔)[1], Jianchen Lu(卢建臣)[1], Cuixia Yan(闫翠霞)[1,†], and Jinming Cai(蔡金明)[1,‡]

[1] *Faculty of Materials Science and Engineering, Kunming University of Science and Technology, Kunming* 650093, *China*
[2] *Institute of Physics, Chinese Academy of Sciences, Beijing* 100190, *China*

(Received 5 November 2018; revised manuscript received 20 December 2018; published online 23 January 2019)

Using first-principle calculations, we predict a new family of stable two-dimensional (2D) topological insulators (TI), monolayer Be_3X_2 (X = C, Si, Ge, Sn) with honeycomb Kagome lattice. Based on the configuration of Be_3C_2, which has been reported to be a 2D Dirac material, we construct the other three 2D materials and confirm their stability according to their chemical bonding properties and phonon-dispersion relationships. Because of their tiny spin–orbit coupling (SOC) gaps, Be_3C_2 and Be_3Si_2 are 2D Dirac materials with high Fermi velocity at the same order of magnitude as that of graphene. For Be_3Ge_2 and Be_3Sn_2, the SOC gaps are 1.5 meV and 11.7 meV, and their topological nontrivial properties are also confirmed by their semi-infinite Dirac edge states. Our findings not only extend the family of 2D Dirac materials, but also open an avenue to track new 2DTI.

Keywords: Dirac materials, topological insulator, first-principles calculation, spin–orbit coupling

PACS: 71.15.Mb, 73.20.At **DOI:** 10.1088/1674-1056/28/3/037101

1. Introduction

Two-dimensional (2D) Dirac materials, with a linear band dispersion around the Fermi level and massless carriers that can be described by Dirac equations,[1,2] displaying ballistic charge transport and enormously high carrier mobility, exhibiting special topological phases,[3–11] will offer potential applications for high performance electronic and spintronic devices. However, the Dirac cores in most of these 2D materials can only exist in the absence of spin–orbit coupling (SOC).[12] The SOC will open a gap at the Dirac point and lead to a topological insulating phase, especially when the SOC strength is very strong.[7,13] The 2D topological insulators (TI) exhibit the quantum spin Hall effect with spin-filtered edge states in their bulk SOC gaps.[14,15] In general, if the SOC gap is very small ($<$ 1 meV, e.g., the SOC gap for graphene is about 0.0008 meV),[16] the influence of the SOC will be neglected, and it will be considered that the 2D material is a "real" 2D Dirac material with linear band dispersion around the Fermi level.[17] If the SOC gap is large ($>$ 1 meV), the 2D Dirac materials will be 2DTI.[18,19] Then, the 2D Dirac materials are more likely composed of light elements (e.g., B, C, N) and the 2DTI are more likely constructed by heavy elements (e.g., Sn, Pb, Bi). Up to now, lots of 2D Dirac materials (or 2DTI) have been predicated and investigated, which include graphene,[1] silicene,[18,20] germanene,[18,20] several kinds of graphynes,[21–23] topological insulators on semiconductor surfaces,[4–6,9–11] 2D organic TI,[6–8] and so on. Especially for graphene, as the only 2D Dirac material that has been truly confirmed in experiment, it has attracted intense interest over the past decade.[1,24]

Graphene, graphynes, and silicene are all single-element materials. Compare to these single-element materials, bi-element materials have more complex structures and more potential to be modulated. Up to now, lots of bi-element 2D Dirac materials and 2DTI have been predicted and investigated, e.g., polyaniline (C_3N),[25] C_4N-I,[25] C_4N-II,[25] TiB_2,[26] and MC_6 (M = Mo, W).[27] Recently, Wang *et al.* have predicted a new 2D Dirac material, monolayer Be_3C_2, by using the global particle-swarm optimization method and density functional theory.[28] We know that the group IV elemental monolayers have played a crucial role in the field of 2D materials, where graphene (C) is a Dirac material, silicene (monolayer Si),[18,20] germanene (monolayer Ge),[18,20] and stanene (monolayer Sn) are topological insulators.[29] Then, what is the stability and electronic properties of the Be_3X_2 (X = Si, Ge, Sn)?

In this work, by using first-principle calculations, we investigated the stability and electronic properties of honeycomb Kagome (HK) mixed 2D materials Be_3X_2 (X = C, Si, Ge, Sn), and found that all of them are 2DTI. More interestingly, mono-

*Project supported by the National Natural Science Foundation of China (Grant Nos. 11674136 and 11564022), the Thousand Talents Plan — the Recruitment Program for Young Professionals, China (Grant No. 1097816002), Yunnan Province for Recruiting High-Caliber Technological Talents, China (Grant No. 1097816002), Reserve Talents for Yunnan Young and Middle-aged Academic and Technical Leaders, China (Grant No. 2017HB010), the Academic Qinglan Project of Kunming University of Science and Technology (KUST), China (Grant No. 1407840010), the Analysis and Testing Fund of KUST, China (Grant No. 2017M20162230010), and the High-level Talents of KUST, China (Grant No. 1411909425).

†Corresponding author. E-mail: j.cai@kmsut.edu.cn
‡Corresponding author. E-mail: cuixiayan09@gmail.com

© 2019 Chinese Physical Society and IOP Publishing Ltd

layer Be_3C_2 and Be_3Si_2 have very tiny SOC gaps (< 1 meV), which means that both are 2D Dirac materials. According to the semi-infinite Dirac edge states of these four materials, we can confirm that Be_3Ge_2 and Be_3Sn_2 are 2DTI, and their SOC gaps are much larger than those of Be_3C_2 and Be_3Si_2.

2. Computational details

The density-functional calculations are performed by using the plane wave basis Vienna *ab initio* simulation pack (VASP).[30] The projector-augmented plane wave (PAW) approach is used to represent the ion–electron interaction.[31] The Perdew–Burke–Ernzerhof (PBE) generalized gradient approximation is adopted for the electron–electron interactions.[32] The energy cutoff of the plane wave is set to 600 eV with a precision energy of 10^{-4} eV/atom and a precision force of.01 eV/Å. The Monkhorst–Pack scheme with $15 \times 15 \times 1$ and $95 \times 95 \times 1$ k-points is used to sample the Brillouin zone for structural optimization and self-constant electronic properties calculation, respectively. In all the calculations, the 18 Å vacuum layer is used to avoid the spurious interactions between periodic images. To assess the dynamical stability, phonon dispersions are calculated based on the finite displacement method which is embedded in the phonopy program.[33,34] The semi-infinite Dirac edge states are calculated by using the Wannier90 package.[35,36]

3. Results and discussion

3.1. Geometrical properties and structural stabilities

A geometrical configuration of monolayer Be_3Si_2 is shown in Fig. 1(a), which has the same lattice as that of Be_3C_2, the HK lattice, where it is composed of a hexagonal lattice formed by the Si atoms and a Kagome lattice formed by the Be atoms. From this figure, we can find that there are three Be and two Si atoms in its unit cell, with a Be–Si bond length of 2.12 Å. Due to sp^2 orbital hybridizations, each Si atom bonds with three Be atoms by using a strong σ-bond, and the final p_z electrons make up the π-bond. In addition, we also calculate the phonon dispersion curves of the monolayer Be_3Si_2, as shown in Fig. 1(b). An absence of imaginary frequencies demonstrates dynamical stabilities of the Be_3Si_2 structure. For Be_3Ge_2 and Be_3Sn_2, both have the same geometrical structure as that of Be_3Si_2, but their lattice constants are different (shown in Table 1), where the bond length of Be–Ge is 2.14 Å, and the bond length of Be–Sn is 2.34 Å. Meanwhile, an absence of imaginary frequencies in the phonon dispersion curves of Be_3Ge_2 and Be_3Sn_2 (Fig. S1) also demonstrates their dynamical stability. We also performed *ab initio* molecular dynamics (MD) simulations using a supercell of 3×3 unit cells at 300 K up to 5 ps and confirmed that these three structures are stable (see Figs. S1(c)–S1(e) in the supporting information). To reveal the bonding nature of monolayer Be_3Si_2, we calculate the electron localization function (ELF),[37,38] which is shown in the right inset of Fig. 1(b). The high ELF value between Be atoms and Si atoms indicates a strong covalent bond between them, which stabilizes the 2D monolayer Be_3Si_2.

Table 1. Lattice constants a, band gaps within SOC E_g, and Fermi velocities V_F of graphene, silicene, and Be_3X_2.

Phase	Graphene	Silicene	Be_3C_2	Be_3Si_2	Be_3Ge_2	Be_3Sn_2
a/Å	2.45	3.83	5.69	7.35	7.42	8.11
E_g/meV	0.0008	1.55	0.04	0.06	1.5	11.7
$V_F/10^5$ m·s^{-1}	8.2	10	4.6	5.7	–	–

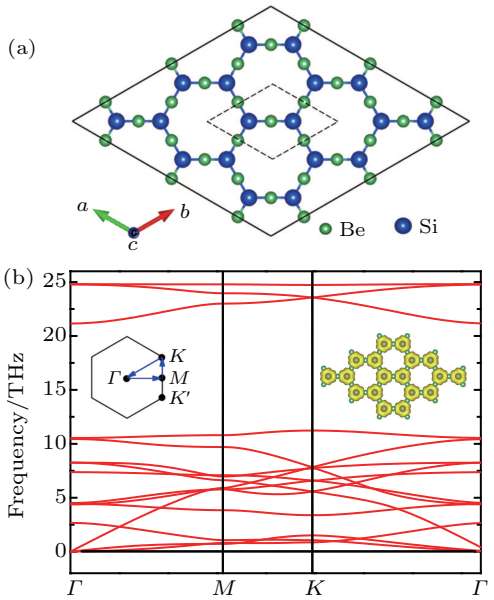


Fig. 1. (a) Optimized configuration of Be_3Si_2 monolayer with a unit cell labeled by black dashed line. The green and blue spheres represent Be and Si, respectively. (b) Phonon-dispersion curves, where the left inset indicates the first Brillouin zone, and the right inset shows the electron localization function of the Be_3Si_2 monolayer with the iso-value of 0.96.

3.2. Electronic properties and Dirac states of Be_3Si_2

To investigate the electronic properties of monolayer Be_3Si_2, we calculate its band structures and corresponding projected density of states (PDOS), as shown in Fig. 2. From its band structure, we can find that there are two linear bands crossing at the Fermi level, which is a typical type of Dirac material, where the Dirac point just locates at the high-symmetry K point. The PDOS shows that the Dirac states near the Fermi level are mainly contributed to by the p_z orbital of Si, which can be indicated by real space charge distributions of the highest occupied band (HOB) and the lowest unoccupied band (LUB) of Be_3Si_2 (Figs. 2(c) and 2(d)). We also provide the three-dimensional valence and conduction bands in Fig. 2(b), which clearly shows the features of the Dirac cone in its first Brillouin zone. The linear dispersion of the energy bands suggests that the effective mass of the carriers near the Fermi level is zero (the effective mass of charge carriers is defined as $m^* = \hbar(\mathrm{d}^2E/\mathrm{d}k^2)^{-1}$). The calculated Fermi velocity is about 5.7×10^5 m/s, and the linear dispersion maintains until about

±0.25 eV away from the Dirac point. Both are close to one-half of that in freestanding graphene.[39] Therefore, the Be_3Si_2 monolayer is expected to have ultra-high carrier mobility and excellent electronic transport properties.

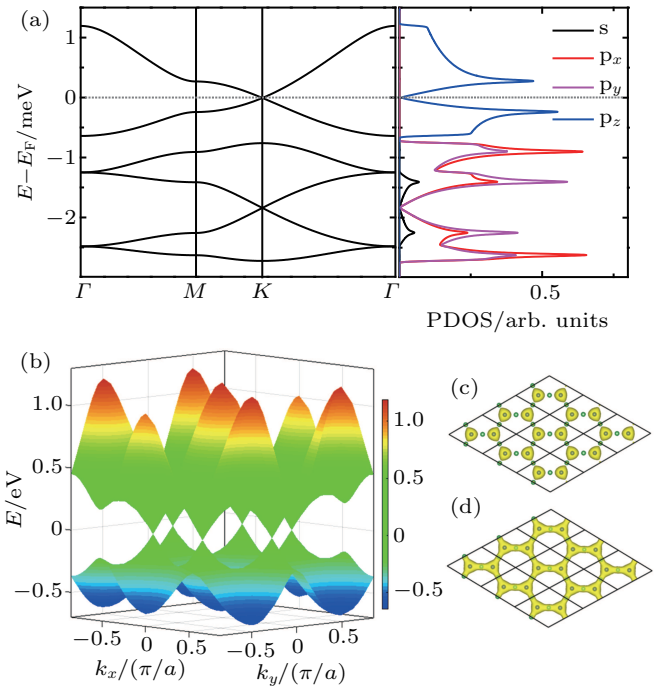


Fig. 2. Electronic structures of Be_3Si_2: (a) band structure and PDOS, (b) 3D valence and conduction bands around the Fermi level, (c) and (d) the real space charge distributions of HOB and LUB.

Mostly, Dirac cores can only exist in the absence of SOC.[12] But Be_3C_2 can be considered as 2D Dirac materials even with SOC, because its SOC gap is very small (0.04 meV).[28] For Be_3Si_2, the SOC can open a tiny band gap of 0.06 meV, being also much smaller than 1 meV, which means that Be_3Si_2 is one new "real" 2D Dirac material. We know that silicene is a 2DTI with a SOC band gap about 1.55 meV.[18] The large SOC gap comes from buckled properties of silicene, where some of the in-plane orbitals contribute to the bands around the Fermi level.[20] Here, there is no buckle for Be_3Si_2, and only the p_z orbitals (out of plane orbitals) of Si contribute to the bands around the Fermi level. Similar to graphene and Be_3C_2, Be_3Si_2 has a very small SOC gap, which leads it to be a 2D Dirac material.

3.3. Topological properties of Be_3X_2

In Fig. 3(a), we provide a zoom-in band structure with SOC of Be_3Si_2 around the Fermi level, where we can clearly find the linear dispersion relationship. To calculate the topological edge states, we firstly fit a tight binding Hamilton based on the largest localized Wannier function (MLWF) according to the DFT band structure.[36] Then, by using the MLWFs, we build the edge Green's function of the semi-unique lattice by using recursive methods and calculate the local density of states (LDOS) (shown in Figs. 3(b), 4(d), and 5(d)).[36] According to our calculation results, we can find that nontrivial topological edge states connect the bulk bands. For Be_3Si_2, due to the tiny SOC gap, the two time-reversal-symmetry bands (Dirac bands of the edge states) around the Fermi level nearly degenerate, and it seems that there is an arc connecting the two Dirac points (Fig. 3(b)). For Be_3Ge_2 and Be_3Sn_2, without SOC, they have similar band structures to that of Be_3Si_2 (Figs. 4(a) and 5(a)). However, with SOC, because the SOC strengths of Ge and Sn are much larger than that of C, their SOC band gaps are 1.5 meV and 11.7 meV, respectively, and both are 2DTI. We also use the HSE06 method to calculate the SOC band gaps of these three structures and find that their band gaps are 0.34 meV, 1.55 meV, and 18.9 meV, respectively. In Figs. 4(c) and 5(c), we provide their zoom-in band structures with SOC around the Fermi level, where we can clearly see the SOC gaps at the Dirac points. In Figs. 4(d) and 5(d), we can clearly find the semi-infinite edge states within the SOC gaps, then we can confirm that that they are both intrinsic 2DTI with larger SOC gaps than Be_3C_2 and Be_3Si_2 (Figs. 4(d) and 5(d)).

More interestingly, for Be_3Sn_2, its deep energy bands exhibit much larger SOC band gaps (~0.2 eV) and semi-infinite Dirac edge states (Fig. S2). These large SOC band gaps mean that we can realize a large gap 2DTI if we move the Fermi level to these gaps by hole doping.

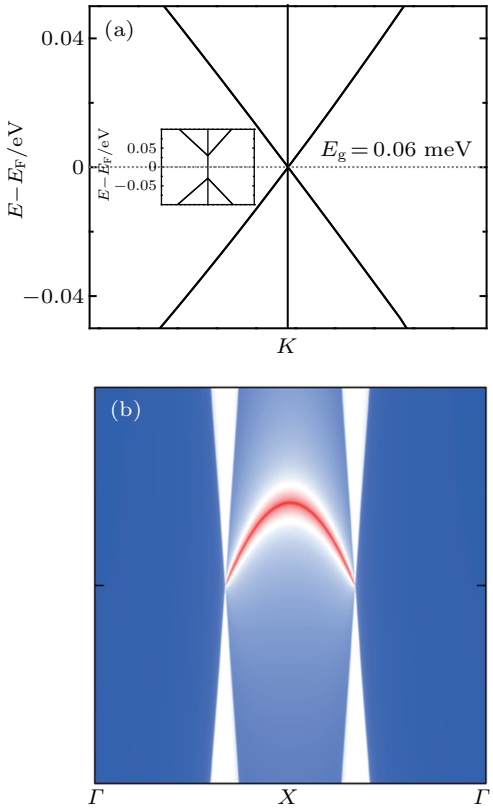


Fig. 3. (a) Band structures of Be_3Si_2 with SOC around K points, where the inset is the zoom-in view around the Fermi level. (b) The semi-infinite Dirac edge states around the Fermi level.

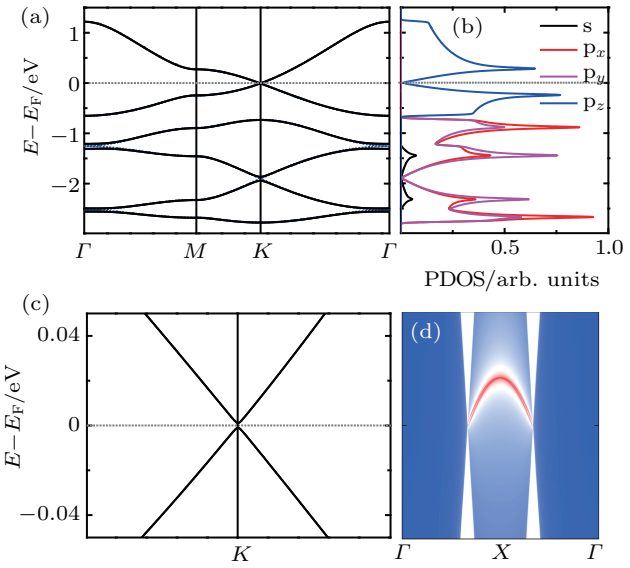


Fig. 4. Electronic properties of Be_3Ge_2. (a) Band structures with (black line) and without (blue dash) SOC. (b) Projected density of states without considering SOC. (c) Zoom-in figure around K points of the band structures considering the SOC. (d) The semi-infinite Dirac edge states around the Fermi level.

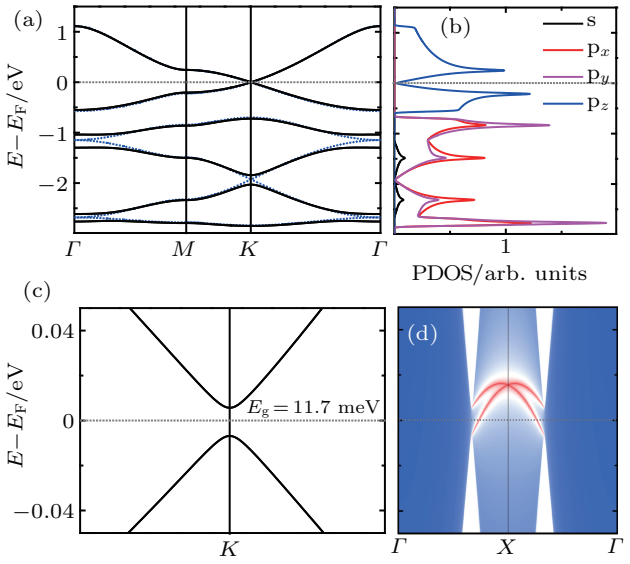


Fig. 5. Electronic properties of Be_3Sn_2. (a) Band structures with (black line) and without (blue dash) SOC. (b) Projected density of states without considering SOC. (c) Zoom-in figure around K points of the band structures considering the SOC. (d) The semi-infinite Dirac edge states around the Fermi level.

4. Conclusion

We investigate a family of 2DTI with HK lattice, monolayer Be_3X_2 (X = C, Si, Ge, Sn). Based on the chemical bonding properties and phonon-dispersion relationships, we have confirmed their stabilities. By investigating their electronic and topological properties, we find that Be_3C_2 and Be_3Si_2 can be considered as 2D Dirac materials because of their tiny SOC band gaps. For Be_3Ge_2 and Be_3Sn_2, the SOC gaps are 1.5 meV and 11.7 meV, and their topological nontrivial properties are also confirmed by their semi-infinite Dirac edge states. Since the atomic numbers of the Ge and Sn atoms are larger than those of the C and Si atoms, the spin–orbit coupling effect is larger. Our research will enrich the family of 2DTI and promote the development of 2D materials.

References

[1] Castro Neto A H, Guinea F, Peres N M R, Novoselov K S and Geim A K 2009 *Rev. Mod. Phys.* **81** 109
[2] Novoselov K 2007 *Nat. Mater.* **6** 720
[3] Wang Z F, Liu Z and Liu F 2013 *Nat. Commun.* **4** 1471
[4] Zhou M, Ming W, Liu Z, Wang Z, Li P and Liu F 2014 *Proc. Natl. Acad. Sci. USA* **111** 14378
[5] Zhu F F, Chen W J, Xu Y, Gao C L, Guan D D, Liu C H, Qian D, Zhang S C and Jia J F 2015 *Nat. Mater.* **14** 1020
[6] Zhang L Z, Zhai F, Jin K H, Cui B, Huang B, Wang Z, Lu J Q and Liu F 2017 *Nano Lett.* **17** 4359
[7] Kane C L and Mele E J 2005 *Phys. Rev. Lett.* **95** 226801
[8] Zhang L Z, Wang Z F, Huang B, Cui B, Wang Z, Du S X, Gao H J and Liu F 2016 *Nano Lett.* **16** 2072
[9] Huang B, Jin K H, Zhuang H L, Zhang L and Liu F 2016 *Phys. Rev. B* **93** 115117
[10] Li P, Zhou M, Zhang L, Guo Y and Liu F 2016 *Nanotechnology* **27** 095703
[11] Chuang F C, Hsu C H, Huang Z Q, Kuo C C, Liu Y T, Lin H and Bansil A 2015 *New J. Phys.* **17** 025005
[12] Young S M and Kane C L 2015 *Phys. Rev. Lett.* **115** 126803
[13] Kane C L and Mele E J 2005 *Phys. Rev. Lett.* **95** 146802
[14] Qi X L and Zhang S C 2011 *Rev. Mod. Phys.* **83** 1057
[15] Schumayer D and Hutchinson D A W 2011 *Rev. Mod. Phys.* **83** 769
[16] Yao Y, Ye F, Qi X L, Zhang S C and Fang Z 2007 *Phys. Rev. B* **75** 041401
[17] Mayorov A S, Elias D C, Mukhin I S, Morozov S V, Ponomarenko L A, Novoselov K S, Geim A K and Gorbachev R V 2012 *Nano Lett.* **12** 4629
[18] Liu C C, Feng W and Yao Y 2011 *Phys. Rev. Lett.* **107** 076802
[19] Dai X 2016 *Physics* **12** 5
[20] Cahangirov S, Topsakal M, Akturk E, Sahin H and Ciraci S 2009 *Phys. Rev. Lett.* **107** 076802
[21] Malko D, Neiss C, Vines F and Goerling A 2012 *Phys. Rev. Lett.* **108** 086804
[22] Xu L C, Wang R Z, Miao M S, Wei X L, Chen Y P, Yan H, Lau W M, Liu L M and Ma Y M 2014 *Nanoscale* **6** 1113
[23] Zhang L Z, Wang Z F, Wang Z M, Du S X, Gao H J and Liu F 2015 *J. Phys. Chem. Lett.* **6** 2959
[24] Cheng H E, Ming-Hui L U and Chen Y F 2008 *Physics* **1** 16
[25] Li L, Kong X, Leenaerts O, Chen X, Sanyal B and Peeters F M 2017 *Carbon* **118** 258
[26] Zhang L Z, Wang Z F, Du S X, Gao H J and Liu F 2014 *Phys. Rev. B* **90** 161402
[27] Liu P F, Wu Y, Bo T, Hou L, Xu J, Zhang H J and Wang B T 2018 *Phys. Chem. Chem. Phys. Pccp* **20** 732
[28] Wang B, Yuan S, Li Y, Shi L and Wang J 2017 *Nanoscale* **9** 5577
[29] Xu Y, Yan B, Zhang H J, Wang J, Xu G, Tang P, Duan W and Zhang S C 2013 *Phys. Rev. Lett.* **111** 136804
[30] Stadler R, Wolf W, Podloucky R, Kresse G, Furthmã¼Ller J and Hafner J 1996 *Phys. Rev. B* **54** 1729
[31] Kresse G and Joubert D 1999 *Phys. Rev. B* **59** 1758
[32] Perdew J P, Burke K and Ernzerhof M 1996 *Phys. Rev. Lett.* **77** 3865
[33] Parlinski K, Li Z Q and Kawazoe Y 1997 *Phys. Rev. Lett.* **78** 4063
[34] Togo A, Oba F and Tanaka I 2008 *Phys. Rev. B* **78** 134106
[35] Mostofi A A, Yates J R, Pizzi G, Lee Y S, Souza I, Vanderbilt D and Marzari N 2014 *Comput. Phys. Commun.* **185** 2309
[36] Wu Q S, Zhang S N, Song H F, Troyer M and Soluyanov A A 2018 *Comput. Phys. Commun.* **224** 405
[37] Becke A D and Edgecombe K E 1990 *J. Chem. Phys.* **92** 5397
[38] Savin A, Jepsen O, Flad J, Andersen O K, Preuss H and Von Schnering H G 1992 *Angew. Chem.* **31** 187
[39] Wallace P R 1947 *Phys. Rev.* **71** 622